J Electr Eng Technol Vol. 9, No. 6: 1921-1927, 2014
http://dx.doi.org/10.5370/JEET.2014.9.6.1921

ISSN(Print) 1975-0102
ISSN(Online) 2093-7423

Magnetic Field Gradient Optimization for Electronic Anti-Fouling Effect in Heat Exchanger

Yong Han* and Shu-tao Wang†

Abstract – A new method for optimizing the magnetic field gradient in the exciting coil of electronic anti-fouling (EAF) system is presented based on changing exciting coil size. In the proposed method, two optimization expressions are deduced based on biot-savart law. The optimization expressions, which can describe the distribution of the magnetic field gradient in the coil, are the function of coil radius and coil length. These optimization expressions can be used to obtain an accurate coil size if the magnetic field gradient on a certain point on the coil's axis of symmetry is needed to be the maximum value. Comparing with the experimental results and the computation results using Finite Element Method simulation to the magnetic field gradient on the coil's axis of symmetry, the computation results obtained by the optimization expression in this article can fit the experimental results and the Finite Element Method results very well. This new method can optimize the EAF system's anti-fouling performance based on improving the magnetic field gradient distribution in the exciting coil.

Keywords: Electronic anti-fouling system, Exciting coil, Magnetic field gradient, Optimization

1. Introduction

The scale problem is a big problem to the devices which have the heat exchange process when they work, such as cooling tower and boiler. The scale problem roots on using hard water. Chemicals were used to prevent scale buildup at first [1-2]. But using chemicals can bring many problems such as environmental contamination. Then the electromagnetic anti-fouling method was researched and used as a substitute. The electronic anti-fouling (EAF) system is a very useful electromagnetic field water treatment system to the scale problem. The structure diagram of EAF system is shown as Fig. 1. When EAF system works, EAF Control Unit will load a high frequency alternate signal to the exciting coil which is winded on the tube. The alternate signal takes a certain power, and the induced electromagnetic field generated by exciting coil treats the mineral solution. But the anti-fouling mechanism of EAF system is still not all clear as yet. So it is scarce of theoretical direction to make a good use of EAF system.

Tombacz E et al [3, 4] studied the effect of a weak magnetic field on hematite sol in stationary and flowing systems. They found that when the flow direction was vertical to the magnetic field direction vector, the cluster of electrolyte particle was formed in the solution. But the cluster of electrolyte particle wasn't observed in the solution which was placed in the static magnetic field. They believed that the cluster of electrolyte particle phenomenon was caused by the lorentz force. According to the Tombacz E's standpoint, there are Ca^{2+}, CO_3^{2-}, Mg^{2+}, SO_4^{2-}, HCO_3^{-} and some other electrolyte particle in the hard water, EAF system can make magnetic field in its exciting coil, therefore all kinds of electrolyte particle can be influenced by lorentz force when the hard water is flowing throw the coil. The lorentz force is a very important reason for magnetic field anti-fouling but not the only reason. The magnetic field gradient (MFG) is another important reason for magnetic field anti-fouling. According to the gradient magnetic separation theory, diamagnetism electrolyte particle or paramagnetism electrolyte particle will be acted on by gradient magnetic force when they are in gradient magnetic field. The gradient magnetic force can be expressed as [5, 6]:

$$\vec{F} = c_0 K_m H \frac{dH}{dz} \tag{1}$$

Where c_0 is an environment constant, K_m is magnetic susceptibility, H is magnetic field intensity, dH/dz is the

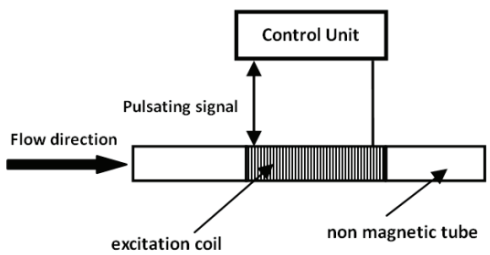

Fig. 1. Structure sketch of the EAF system.

† Corresponding Author: Detp. of Measurement Technology and Instrumentation Key Laboratory of Hebei Province, School of Electrical Engineering, Yanshan University. Qinhuangdao, China. (wangshutao@ysu.edu.cn)
* Detp. of Measurement Technology and Instrumentation Key Laboratory of Hebei Province, School of Electrical Engineering, Yanshan University. Qinhuangdao, China. (hanyong_hit@163.com)
Received: January 8, 2014; Accepted: April 21, 2014

gradient of magnetic field. In the hard water, it is known that Ca^{2+} and Mg^{2+} are diamagnetism, but CO_3^{2-}, HCO_3^- and SO_4^{2-} are paramagnetism according to Van Vleck's theory [7, 8]. Therefore the direction of gradient magnetic force acting on Ca^{2+} and Mg^{2+} is opposite with the direction of gradient magnetic force acting on CO_3^{2-}, HCO_3^- and SO_4^{2-}. Therefore the negative ions and positive ions are formed into clusters respectively, and the clusters in the solution can become many seeds of the scale crystal. Then the scale crystal can grow up in the hard water solution instead of growing on the water tube wall. Some researchers found that the anti-fouling effect caused by gradient magnetic field was much better than the anti-fouling effect caused by uniform magnetic field [9, 10]. Therefore the anti-fouling performance of EAF system can be optimized by making a biggest magnetic field gradient in the exciting coil.

The magnetic field in the coil is not uniform, and the ratio of coil radius to coil length can influence the magnetic field gradient in the exciting coil. On the same cross section which is vertical with the axis of symmetry of the coil, magnetic field gradient is almost the same. In addition, the axial component of the magnetic field is much bigger than the radial component of the magnetic field, and the tangential component of the magnetic field is zero. Therefore in the present study the axial magnetic field gradient on the axis of symmetry of exciting coil will be optimized by changing the ratio of coil radius to coil length.

2. Optimization Method Modeling

In this paper the exciting coil is single layer for a tightly wound. The cross profile schematic diagram of the coil is shown as Fig. 2. In Fig. 2, $2l$ is the coil length, r is coil radius, z is the distance between a certain point on the coil's axis of symmetry and the central point of the coil.

The computational formula of the magnetic field intensity on the coil's axis of symmetry is as [11]:

$$H_z = \frac{B_z}{\mu_0} = \frac{nI}{2}\left[\frac{(l+z)}{\sqrt{r^2+(l+z)^2}} + \frac{(l-z)}{\sqrt{r^2+(l-z)^2}}\right] \quad (2)$$

where H_z is the axial magnetic field intensity, B_z is the axial magnetic induction intensity, μ_0 is vacuum permeability, I is the exciting electric current, n is the number of turns per unit length of the coil. Then the H_z's derivative with respect to z is as:

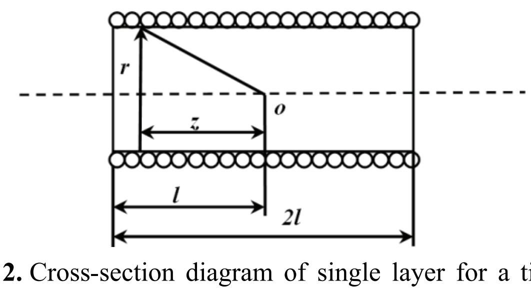

Fig. 2. Cross-section diagram of single layer for a tightly wound solenoid.

$$\frac{\mathrm{d}H_z}{\mathrm{d}z} = \frac{nI}{2}\left\{\frac{r^2}{[r^2+(l+z)^2]^{\frac{3}{2}}} - \frac{r^2}{[r^2+(l-z)^2]^{\frac{3}{2}}}\right\} \quad (3)$$

It can be known from Eq. (3) that $\mathrm{d}H_z/\mathrm{d}z$ is the function of r, l and z. When z=0, $\mathrm{d}H_z/\mathrm{d}z$ is 0. Therefore the magnetic field gradient on the midpoint of the coil's axis of symmetry is always 0. It also can be known from Eq. (3) that $\mathrm{d}H_z/\mathrm{d}z$'s maximum value can be calculated only when z is a certain constant. In the present article we set that $z<l$. If the ratio of coil radius to coil length is wanted when magnetic field gradient on a certain constant z is maximum value, the optimization expression should be deduced under two conditions: when the coil length $2l$ is a constant or coil radius r is a constant.

2.1 When the coil length 2*l* is a constant

When the coil length $2l$ is a constant, assume $\alpha = \frac{r}{l}$, then Eq. (3) can be changed into:

$$\frac{\mathrm{d}H_z}{\mathrm{d}z} = \frac{nI}{2}\left\{\frac{\alpha^2}{[\alpha^2+(1+\frac{z}{l})^2]^{\frac{3}{2}}} - \frac{\alpha^2}{[\alpha^2+(1-\frac{z}{l})^2]^{\frac{3}{2}}}\right\} \quad (4)$$

Eq. (4) is the function of α, assume $F(\alpha) = \frac{\mathrm{d}H_z}{\mathrm{d}z}$, $M = \frac{nI}{2l}$, $c = \frac{z}{l}$, then $\frac{\mathrm{d}H_z}{\mathrm{d}z}$'s derivative with respect to α is as:

$$\frac{\mathrm{d}F(\alpha)}{\mathrm{d}\alpha} = 2M\alpha\left[\frac{1}{[\alpha^2+(1+c)^2]^{\frac{3}{2}}} - \frac{1}{[\alpha^2+(1-c)^2]^{\frac{3}{2}}}\right] - 3M\alpha^3\left\{\frac{1}{[\alpha^2+(1+c)^2]^{\frac{5}{2}}} - \frac{1}{[\alpha^2+(1-c)^2]^{\frac{5}{2}}}\right\} \quad (5)$$

$$\Rightarrow \frac{2(1+c)^2-\alpha^2}{[\alpha^2+(1+c)^2]^{\frac{5}{2}}} - \frac{2(1-c)^2-\alpha^2}{[\alpha^2+(1-c)^2]^{\frac{5}{2}}} = 0 \quad (6)$$

Then we can obtain the ratio of coil radius to coil length by solving Eq. (6) when $\mathrm{d}H_z/\mathrm{d}z$ is maximum value.

2.2 When the coil radius *r* is a constant

When the coil radius r is a constant, assume $\beta = \frac{l}{r}$, then Eq. (3) can be changed into:

$$\frac{\mathrm{d}H_z}{\mathrm{d}z} = \frac{nI}{2}\left\{\frac{1}{[1+(\beta+\frac{z}{r})^2]^{\frac{3}{2}}} - \frac{1}{[1+(\beta-\frac{z}{r})^2]^{\frac{3}{2}}}\right\} \quad (7)$$

Eq. (4) is the function of β, assume $G(\beta) = \frac{\mathrm{d}H_z}{\mathrm{d}z}$, $N = \frac{nI}{2r}$, $c = \frac{z}{r}$, then $\frac{\mathrm{d}H_z}{\mathrm{d}z}$'s derivative with respect to β is as:

$$\frac{dG(\beta)}{d\beta} = N\left\{\frac{3(\beta+d)}{[1+(\beta+d)^2]^{\frac{5}{2}}} - \frac{3(\beta-d)}{[1+(\beta-d)^2]^{\frac{5}{2}}}\right\} \quad (8)$$

$$\Rightarrow \quad \frac{\beta+d}{[1+(\beta+d)^2]^{\frac{5}{2}}} - \frac{\beta-d}{[1+(\beta-d)^2]^{\frac{5}{2}}} = 0 \quad (9)$$

Then we can obtain the ratio of coil radius to coil length by solving Eq. (9) when dHz/dz is maximum value.

3. Result Simulation Verification and Discussion

3.1 Simulation verification for Eq. (6)

We set 2l =0.2m, electric current density of the coil is 1250000 A/m^3, n=500/m, and z is 0.02m, 0.05m and 0.08m. In order to verifying the correctness of Eq. (6), first we use Eq. (6) to calculate the maximum value of dH_z/dz and ratio of coil radius to coil length when dH_z/dz is maximum value. Then we use Finite Element Method to calculate the value of dH_z/dz when the ratio of coil radius to coil length is different, and find the maximum value of dH_z/dz and find the ratio of coil radius to coil length when dH_z/dz is maximum.

The Finite Element calculation is done by using Ansys 10.0 software, which has powerful computing capability based on the FEM (finite element method). It can do an accurate calculation of eddy current, inductance, magnetic field intensity and so on [12]. PLANE53 element is used in building the model. PLANE53 is defined by 8 nodes and has up to 4 degrees of freedom (DOF) per node. These DOFs are viz. the z-component of the magnetic vector potential (AZ), the time-integrated electric scalar potential (VOLT), the electric current (CURR), and the electromotive force (emf) [12].

When using Eq. (6), the calculating result is shown as Table 1.

Table 1. MFG maximum and the corresponding ratio of r to l when z=0.02m, 0.05m and 0.08m.

	z=0.02m	z=0.05m	z=0.08m
$\frac{r}{l}$	0.786	0.619	0.280
$\frac{dH_z}{dz}_{max}$ (A / m^2)	2858.4	8385.6	23893.0

Table 2. MFG maximum with different ratio of r to l when z=0.02m

$\frac{r}{l}$	0.1	0.2	0.3	0.4	0.5
$\frac{dH_z}{dz}_{max}$ (A / m^2)	181.57	650.47	1178.8	1763.9	2273.9
$\frac{r}{l}$	0.6	0.7	**0.786**	0.8	0.9
$\frac{dH_z}{dz}_{max}$ (A / m^2)	2643.4	2828.7	**2873.8**	2861.9	2811.2

When using Finite Element Method, the calculating result is shown as Tables 2 - Table 4, and the fitting curves of the results is shown as Figs. 3 - Fig. 5.

It can be seen from Table 1 and Figs (3-5) that the

Table 3. MFG maximum with different ratio of r to l when z=0.05m

$\frac{r}{l}$	0.1	0.2	0.3	0.4	0.5
$\frac{dH_z}{dz}_{max}$ (A / m^2)	926.78	3101.6	5303.4	7144.2	8029.8
$\frac{r}{l}$	0.6	**0.619**	0.7	0.8	0.9
$\frac{dH_z}{dz}_{max}$ (A / m^2)	8392.5	**8476.5**	8275.6	7930.4	7438.4

Table 4. MFG maximum with different ratio of r to l when z=0.08m

$\frac{r}{l}$	0.1	0.2	**0.280**	0.3	0.4
$\frac{dH_z}{dz}_{max}$ (A / m^2)	11656	22419	**24430**	24271	22192
$\frac{r}{l}$	0.5	0.6	0.7	0.8	0.9
$\frac{dH_z}{dz}_{max}$ (A / m^2)	19515	17180	14972	13101	11588

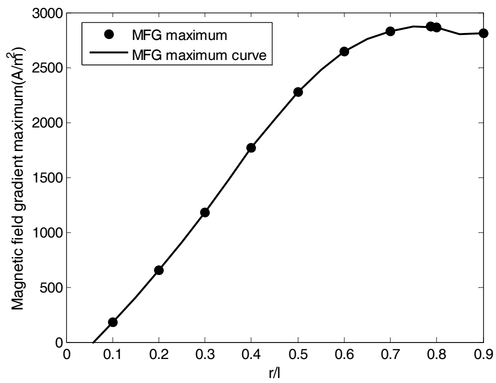

Fig. 3. Fitting curve of MFG maximum with different ratio of r to l when z=0.02m

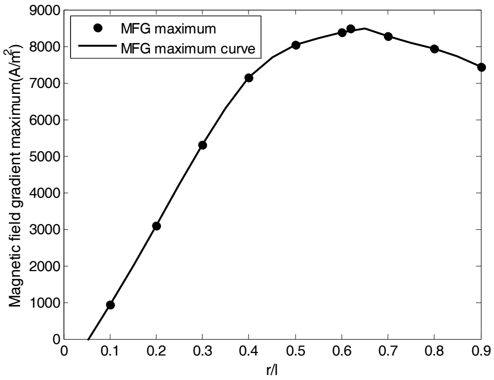

Fig. 4. Fitting curve of MFG maximum with different ratio of r to l when z=0.05m

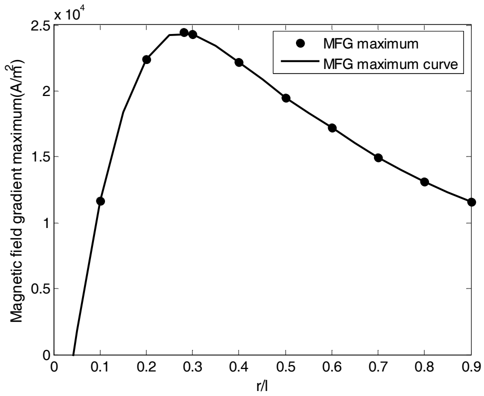

Fig. 5. Fitting curve of MFG maximum with different ratio of r to l when z=0.08m

Table 5. MFG maximum and the corresponding ratio of l to r when z=0.02m, 0.05m and 0.08m.

	z=0.02m	z=0.05m	z=0.08m
$\frac{r}{l}$	0.520	0.648	0.860
$\frac{dH_z}{dz}_{max}$ (A/m^2)	4118.6	8558.0	10715.0

Table 6. MFG maximum with different ratio of l to r when z=0.02m

$\frac{r}{l}$	0.1	0.2	0.3	0.4	0.5
$\frac{dH_z}{dz}_{max}$ (A/m^2)	1296.9	2470.7	3308.7	3858.6	4047.3
$\frac{r}{l}$	**0.520**	0.6	0.7	0.8	0.9
$\frac{dH_z}{dz}_{max}$ (A/m^2)	**4094.1**	4037.3	3811.9	3473.9	3019.0

Table 7. MFG maximum with different ratio of l to r when z=0.05m

$\frac{r}{l}$	0.1	0.2	0.3	0.4	0.5
$\frac{dH_z}{dz}_{max}$ (A/m^2)	2103.1	4074.1	5784.7	7152.4	8196.3
$\frac{r}{l}$	0.6	**0.648**	0.7	0.8	0.9
$\frac{dH_z}{dz}_{max}$ (A/m^2)	8435.7	**8532.2**	8441.0	8131.2	7554.9

Table 8. MFG maximum with different ratio of l to r when z=0.08m

$\frac{r}{l}$	0.1	0.2	0.3	0.4	0.5
$\frac{dH_z}{dz}_{max}$ (A/m^2)	1737.9	3461.6	5130.1	6696.2	8121.2
$\frac{r}{l}$	0.6	0.7	0.8	**0.860**	0.9
$\frac{dH_z}{dz}_{max}$ (A/m^2)	9300.7	10127	10567	**10690**	10626

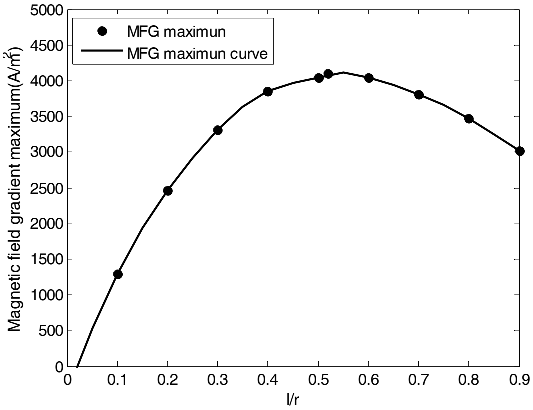

Fig. 6. Fitting curve of MFG maximum with different ratio of l to r when z=0.02m

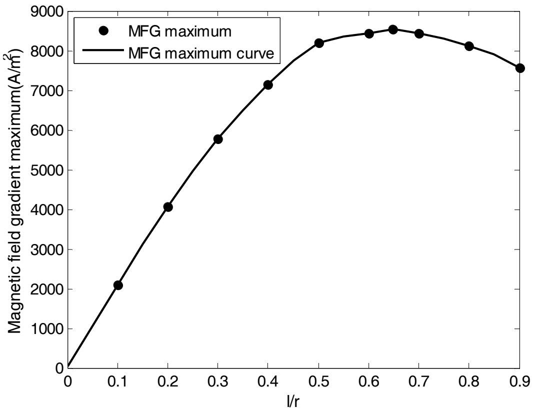

Fig. 7. Fitting curve of MFG maximum with different ratio of l to r when z=0.05m

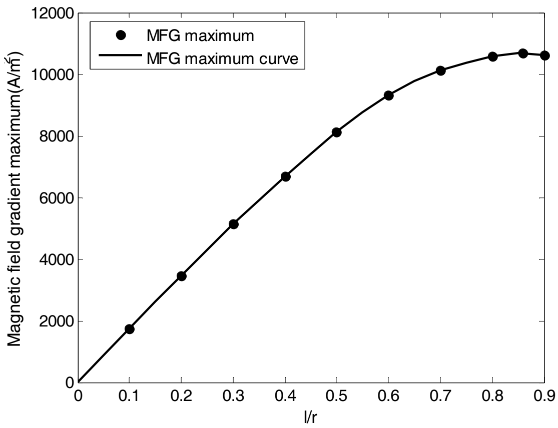

Fig. 8. Fitting curve of MFG maximum with different ratio of l to r when z=0.08m

results calculated by Eq. (6) can fit well with finite element calculation results. Therefore the correctness of Eq. (6) is verified.

3.2 Simulation verification for Eq. (9)

We set r=0.1m, electric current density of the coil is

1250000 A/m^3, n=500/m, and z is 0.02m, 0.05m and 0.08m. In order to verifying the correctness of Eq. (6), first we use Eq. (9) to calculate the maximum value of dH_z/dz and ratio of coil radius to coil length when dH_z/dz is maximum value. Then we use Finite Element Method to calculate the value of dH_z/dz when the ratio of coil radius to coil length is different, and find the maximum value of dH_z/dz and find the ratio of coil radius to coil length when dH_z/dz is maximum. When using Eq. (9), the calculating result is shown as Table 5.

When using Finite Element Method, the calculating result is shown as Table 6 - Table 8, and the fitting curves of the results is shown as Fig. 6 - Fig. 8.

It can be seen from Table 5 and Figs (6-8) that the results calculated by Eq. (9) can fit well with finite element calculation results. Therefore the correctness of Eq. (9) is verified.

3.3 Experimentation Verification for Eqs. (6) and Eq. (9)

In the present study the validity of Eqs. (6) and Eq. (9) was also verified experimentally.

We made the coils with different size according to the Finite Element models which were built in the section A and section B of part III above. The exciting coil was made up by copper wire, and the resistivity of the copper wire was 1.7×10^{-8} (Ω・m) when ambient temperature was 25℃. The diameter of the copper wire was 0.002m. The exciting electric current was 1.25 A. The magnetic field gradient on the axis of exciting was measured with a weak magnetic field gradient meter (produced by Beijing Zhong Hui Tian Cheng technology co., LTD). The weak magnetic field gradient meter's highest resolution was 0.01μT, and its recording sensitivity and registration accuracy were 0.004 μT/cm and ±0.25% respectively. The experimental setup is shown in Fig. 9.

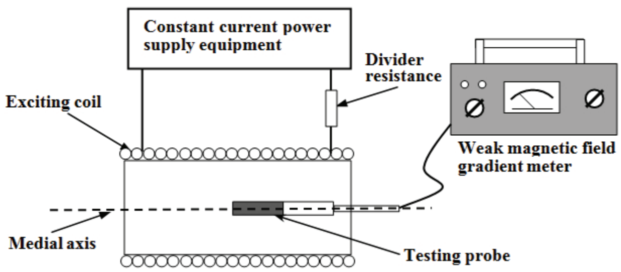

Fig. 9. Schematic diagram of experimental setup

The experiment was divided into two stages.

3.3.1 Stage 1

First we let the length of exciting coil as a constant: 2l= 0.2m, and we changed the coil's radius from 0.01m to 0.1m. The magnetic field gradient on the axis point of z=0.02m (z is the distance from the medial point of axis) was measured under different coil radius, and the corresponding coil radius was found out when the magnetic field gradient on the axis point of z was maximum. At last the maximum magnetic field gradient value was recorded.

Then we changed the axis points of z=0.05m and z=0.08m and repeated the experimental steps above.

Table 9. The experiment results of stage 1

	z=0.02m	z=0.05m	z=0.08m
r (m)	0.078	0.063	0.027
$\frac{r}{l}$	0.78	0.63	0.27
$\frac{dH_z}{dz}_{max}$ (A / m^2)	2872	8403	23916

3.3.2 Stage 2

First we let the radius of exciting coil as a constant: r= 0.1m, and we changed the coil's length from 0.01m to 0.1m. The magnetic field gradient on the axis point of z=0.02m was measured under different coil length, and the corresponding coil length was found out when the magnetic field gradient on the axis point of z was maximum. At last the maximum magnetic field gradient value was recorded.

Then we changed the axis points of z=0.05m and z=0.08m and repeated the experimental steps above.

Table 10. The experiment results of stage 2

	z=0.02m	z=0.05m	z=0.08m
l (m)	0.053	0.064	0.088
$\frac{r}{l}$	0.53	0.64	0.88
$\frac{dH_z}{dz}_{max}$ (A / m^2)	4139	8572	10735

The unit of maximum magnetic field gradient value measured by weak magnetic field gradient meter was transformed from μT /cm into A/m^2 according to Eq. (10).

$$B=\mu_0 H \qquad (10)$$

where B is magnetic induction intensity (the SI unit is T) and H is magnetic field intensity (the SI unit is A/m). μ_0 is vacuum permeability. The experimental results are shown in Tables 9 and Table 10.

It can be seen from Tables 9 and Table 10 that experiment results can fit well with the results calculated by Eqs. (6) and Eq. (9) which are shown in Tables 1 and Table 5.

3.4 Discussion

1) According to Eq. (1), the magnetic field gradient is inversely proportional to magnetic field intensity when $\vec{F}$ is a constant. The magnetic field gradient is bigger when the magnetic field intensity is smaller. The magnetic

field intensity is proportional to the exciting current. In the present paper we obtain a mathematical method to optimize the magnetic field gradient in exciting coil. It means that a small exciting current can obtain a big magnetic field gradient, which means a good anti-fouling effect.

2) The method to optimize the magnetic field gradient in exciting coil in the present paper can be used to make a good anti-fouling effect in the wanted area in the water tube or the heat exchanger. It is helpful for some area in the water circulation system which is hard to clear.

3) In this paper the exciting coil is single layer for a tightly wound. This kind of coil is widespread used in many field. Therefore the optimization method can be used in some field that the magnetic field gradient in the coil is needed to be controlled accurately.

4. Conclusion

In this paper a mathematical method to optimize the magnetic field gradient in exciting coil is presented for giving a theoretical basis to the optimization design of exciting coil of EAF system, and the correctness of the expressions, which are used to calculate the magnetic field gradient maximum, is verified by Finite Element Method and experimentation. This optimization method can be used to make a biggest magnetic field gradient in the certain area in the coil and improve the EAF system's anti-fouling performance by calculating the appropriate ratio of coil radius to coil length. This optimization method can also be used in other coil-using field which the magnetic field gradient is needed to be optimized.

Acknowledgment

This work was financially supported by the National Natural Science Foundation of China (Grant No. 51408525), National Natural Science Foundation of China (Grant No. 61201110), the Specialized Research Foundation for the doctoral program of higher education of China (Grant No. 20101333120004) and Natural Science Foundation of Hebei Province (Grant No.F2014203224).

References

[1] F.C. Nachod and J.Schubert, "Ion Exchange Technology", Academic Press, New York, pp. 10, 1956.

[2] D.L. Owens, "Practical Principles of Ion Exchange Water Treatment", Tall Oaks Publishing, Littleton, CO, pp. 15, 1985.

[3] E. Tombacz, C. Ma, K. W, Busch, et al, "Effect of a Weak Magnetic Field on Hematite Sol in Stationary and Flowing systems", Colloid Polym. Sci, vol. 269, pp. 278-289, 1991.

[4] A. Jedlovszky-Hajdú, E. Tombácz, I. Bányai, et al, "Carboxylated magnetic nanoparticles as MRI contrast agents: Relaxation measurements at different field strengths", Journal of Magnetism and Magnetic Materials, Vol. 324, no. 19, pp. 3173-3180, Sep. 2012.

[5] X Wang, J Zhao, Y Hu, et al, "Effects of the Lorentz force and the gradient magnetic force on the anodic dissolution of nickel in HNO_3+NaCl solution", Electrochimica Acta, Vol. 117, no. 20, pp. 113-119, Jan. 2014.

[6] S K Baik, D W Ha, J M Kwon, et al, "Magnetic force on a magnetic particle within a high gradient magnetic separator", Physica C: Superconductivity, Vol. 484, no. 15, pp. 333-337, Jan. 2013.

[7] Szmytkowski and Radoslaw, "Larmor diamagnetism and Van Vleck paramagnetism in relativistic quantum theory: The Gordon decomposition approach", Physical Review A - Atomic, Molecular, and Optical Physics, vol. 65, no. 3 A, pp. 032112/1-032112/8, March. 2002.

[8] E. Talik, M. Szubka, M. Kulpa, et al, "Van Vleck paramagnetism in lead ytterbium niobate and tantalate single crystals", Journal of Crystal Growth, Vol. 318, no. 1, pp. 874-878, March. 2011.

[9] L.Y. Qi, X.F. Zhang and Y.H. Li, "Effects of frequency on $CaCO_3$ scale by low frequency high gradient magnetic field", Journal of Inner Mongolia University of Science and Technology, vol. 27, no. 3, pp. 271-273, 2008.

[10] X. F. Zhang, G. Y. Liu, D. Q. Cang, C. Y. Song and T.C. Sun, "Mechanism of High-Gradient Magnetic Treatment of Circulating Cooling Water", Iron and Steel, vol. 41, no. 9, pp. 82-84, 2006.

[11] C.S. Li, G.S. Ling, Y. Wang and C.L. Li, "The Optimization of the Uniformity of the Solenoid Magnetic Field", Journal of National University of Defense Technology, vol. 17, no. 2, pp. 90-93, 1995.

[12] S. D. Kore, P. Dhanesh, S. V. Kulkarni and P. P. Date, "Numerical modeling of electromagnetic welding", International Journal of Applied Electromagnetics and Mechanics, vol. 32, no. 1, pp. 1-19, 2010.

Yong Han. He received his B.S. and M.S. degrees from Harbin Institute of Technology, Harbin, China, in 2003 and 2008, respectively and the Ph.D. degree in Instrument Science and Technology also from Institute of Technology in 2013. His research interests are applied electromagnetics and electronic anti-fouling technology.

Shu-tao Wang. He received his B.S. and M.S. degrees from Yanshan University, Qinhuangdao, China, in 1999 and 2002, respectively. He received his Ph.D. degree in Instrument Science and Technology from Institute of Technology, Harbin, China, in 2006. His research interests are weak signal detection and processing and mechanical fault diagnosis.